

Self-similar scaling in decaying numerical turbulence

Tarek A. Yousef*

Department of Energy and Process Engineering, Norwegian University of Science and Technology, Kolbjørn Hejes vei 2B, N-7491 Trondheim, Norway

Nils Erland L. Haugen†

Department of Physics, The Norwegian University of Science and Technology, Høyskoleringen 5, N-7491 Trondheim, Norway

Axel Brandenburg‡

NORDITA, Blegdamsvej 17, DK-2100 Copenhagen Ø, Denmark

(Dated: May 22, 2019, Revision: 1.82)

Decaying turbulence is studied numerically using as initial condition a random flow whose shell-integrated energy spectrum increases with wavenumber k like k^q . Alternatively, initial conditions are generated from a driven turbulence simulation by simply stopping the driving. It is known that the dependence of the decaying energy spectrum on wavenumber, time, and viscosity can be collapsed onto a unique scaling function that depends only on two parameters. This is confirmed using three-dimensional simulations and the dependence of the scaling function on its two arguments is determined.

I. INTRODUCTION

Hydrodynamical turbulence is an example of a system that is self similar, i.e. the velocity pattern looks similar when viewed at different degrees of magnification [1]. Two different self-similarity behaviors have been discussed in the literature: inertial range self-similarity and infrared asymptotic self-similarity that we shall be concerned with here. Most famous is probably the inertial range self-similarity. Kolmogorov [2] showed that the velocity difference between two points, δv , increases with scale ℓ such that $\langle \delta v \rangle \propto \ell^h$, where $h = 1/3$; see also Ref. [3]. In other words, when looking at the velocity at a magnified scale, $\mathbf{x} \rightarrow \alpha \mathbf{x}$, where α is the magnification factor, then velocities will only be similar if they are rescaled by a factor α^h , i.e. $\mathbf{v} \rightarrow \alpha^h \mathbf{v}$.

However, at sufficiently small scales, viscous dissipation always destroys the self-similarity. This implies that there will be a modification to an otherwise perfect power-law behavior of the shell integrated energy spectrum, $E(k)$. This modification can be described by a universal scaling function $\psi(k, \nu)$, which depends on the kinematic viscosity ν . Thus, one can write

$$E(k, \nu) = k^q \psi(k, \nu) \quad (\text{forced turbulence}), \quad (1)$$

where $q = -(1 + 2h)$ follows from the normalization $\int E(k, \nu) dk = \frac{1}{2} \langle v^2 \rangle$. For sufficiently large Reynolds numbers, the energy spectrum has an inertial range with $h = 1/3$, i.e. $q = -5/3$. This spectrum cuts off at the wavenumber $k_d = (\epsilon/\nu^3)^{1/4}$, where ϵ is the rate of energy input. This dependence on ν can be used to simplify the

scaling function to a function that has only one argument, i.e.

$$\psi(k, \nu) = f(k/k_d) = f(k\nu^{3/4}\epsilon^{-1/4}). \quad (2)$$

Here, f is a universal function that depends, in addition to k , only on the outer scale determined by the geometry of the system.

We now discuss the infrared asymptotic self-similarity, i.e. in the following the scaling exponents h and q apply no longer to the inertial range, but to the subinertial (infrared) range. In the case of decaying turbulence, the scaling function also depends on time, i.e. $\psi = \psi(k, t, \nu)$. Furthermore, ψ is not a priori universal in the sense that its form may depend on the initial spectrum. The spectrum also becomes time dependent,

$$E(k, t, \nu) = k^q \psi(k, t, \nu) \quad (\text{decaying turbulence}), \quad (3)$$

where q depends on the initial condition. If the initial condition is restricted to be turbulent so that, prior to turning off the forcing, the energy spectrum satisfies Eq. (1) q is expected to be somewhere between 1 and 4; see Ref. [4, 5].

In a recent paper [7], Ditlevsen, Jensen, and Olesen found that the scaling function $\psi(k, t, \nu)$ reduces to a two-parametric dependence,

$$\psi(k, t, \nu) = g(kt^a, \nu t^b), \quad (4)$$

where $g = g(x, y)$ is a new scaling function that has only two arguments, and a and b are exponents that depend only on the slope of the infrared part of the initial spectrum.

Using data from decaying wind tunnel turbulence [6] it was possible to show [7] that the energy spectra for different times can be collapsed onto a single graph by plotting $k^{-q}E(k, t, \nu)$ versus kt^a . The dependence on the viscosity ν , and hence on the second argument y of the

*Electronic address: Tarek.Yousef@mtf.ntnu.no

†Electronic address: Nils.Haugen@phys.ntnu.no

‡Electronic address: Brandenb@nordita.dk

scaling function $g(x, y)$, has been discarded. This may be appropriate in the large Reynolds number limit.

The purpose of the present paper is to determine, using numerical simulations, the dependence of $g(x, y)$ on both x and y . In a first step we determine the dependence on x by keeping y constant. This is accomplished by letting ν vary in such a way that $\nu t^b \equiv y = \text{const}$. This can obviously not easily be done in wind tunnel turbulence (although ν could in principle be changed by varying the temperature). In a simulation, changing ν is of course quite straightforward. The dependence on y is determined by integrating over x and considering the decay law of kinetic energy.

II. SCALING IN DECAYING TURBULENCE

We first recapitulate the derivation presented in Ref. [7]. The unforced incompressible Navier-Stokes equation,

$$\frac{\partial \mathbf{v}}{\partial t} + \mathbf{v} \cdot \nabla \mathbf{v} + \frac{1}{\rho} \nabla p = \nu \nabla^2 \mathbf{v} \quad (5)$$

where p is pressure, are invariant under the transformation

$$\mathbf{x} \rightarrow \alpha \mathbf{x}, \quad \mathbf{v} \rightarrow \alpha^h \mathbf{v}, \quad t \rightarrow \alpha^{1-h} t, \quad \nu \rightarrow \alpha^{1+h} \nu. \quad (6)$$

In order that Eq. (4) can be satisfied, the exponents a and b have to take certain values. These exponents can be determined by requiring that kt^a and νt^b remain invariant under the scaling transformation (6), i.e.

$$kt^a \rightarrow (\alpha^{-1}k)[\alpha^{(1-h)}t]^a = kt^a, \quad \text{so} \quad a = \frac{1}{1-h}, \quad (7)$$

$$\nu t^b \rightarrow (\alpha^{1+h}\nu)[\alpha^{(1-h)}t]^b = \nu t^b, \quad \text{so} \quad b = -\frac{1+h}{1-h}. \quad (8)$$

Translating this into a dependence on q we have, using $q = -(1+2h)$ and hence $h = -(q+1)/2$,

$$a = \frac{2}{3+q}, \quad b = -\frac{1-q}{3+q}. \quad (9)$$

Note that $b = 0$ for $q = 1$, i.e. for initial energy spectra that increase linearly with k . In Table I we have listed the scaling parameters for several values of q .

The limit $t \rightarrow 0$ is problematic. For $q > 1$, i.e. $b > 0$, both arguments of $g(x, y)$ vanish. Assuming that $g(0, 0)$ is finite, we can conclude that for $t \rightarrow 0$ the dependence of $g(kt^a, \nu t^b)$ on ν and k vanishes. This implies that the zero point of t corresponds to a time where the energy spectrum would have been a pure power law,

$$E(k, 0, \nu) \sim k^q. \quad (10)$$

Such a spectrum is obviously singular and would have infinite energy. We therefore refer to $t = 0$ as a virtual

q	h	a	b	$2n$
1	-1.0	1/2	0	1.00
1.5	-1.25	4/9	1/9	1.11
2	-1.5	2/5	1/5	1.20
3	-2.0	1/3	1/3	1.33
4	-2.5	2/7	3/7	1.43

TABLE I: Dependence of secondary scaling parameters on the slope q of the initial spectrum. The significance of $2n$ will be explained in § III D.

zero point. Near $t = 0$ the spectrum can therefore not be self-similar. On the other hand, if $g(x, y)$ is not necessarily finite in the limit $y \rightarrow 0$, the above conclusion cannot be made. We return to this in § III D. In the following we consider the case where time is sufficiently far away from zero.

The validity of Eqs (3) and (4) has already been confirmed using data from wind tunnel experiments [6] where the viscosity is low enough so that the second argument in $g(x, y)$, $y = \nu t^b$, can be neglected. One goal of the present paper is to demonstrate, using direct simulations, that Eq. (4) is also valid in the case where the second argument, νt^b , cannot be neglected. We do this by implementing in a numerical simulation a time-dependent viscosity, $\nu = \nu(t)$, such that $\nu t^b = \text{const}$ for a given value of the initial power-law exponent q .

As a first test of the scaling relationship we consider the decay of fields with initial power law spectra; see Eq. (10). We will then also test the scaling laws for initial energy spectra that are not power laws (§ III E).

III. COMPARISON WITH SIMULATIONS

The Navier-Stokes equations for an isothermal and weakly compressible fluid are solved in a box with periodic boundary conditions. We always adopt initial velocity fields such that their Mach number is around 1%, so compressibility effects can be neglected. We employ the Pencil Code [8] which is a higher-order finite-difference code using the $2N$ -RK3 scheme of Williamson [9] for time-stepping. The low Re runs presented in this paper were done on relatively coarse grids (64^3) while the high Re runs had a resolution of 256^3 . For further details and recent turbulence simulations using the Pencil Code see Ref. [10]. We begin by studying the evolution of initial velocity fields with power-law spectra.

A. Initial power-law spectra

The initial power-law spectra with arbitrary values of q are constructed by first generating in real space a random velocity field that is delta-correlated in space. Such a velocity field corresponds to a k^2 energy spectrum. In

Fourier space, the velocity field, $\hat{v}(\mathbf{k})$, is then multiplied by a factor $k^{q/2-1}$.

In the upper panel of Fig. 1 we show the results of a numerical experiment where a power spectrum with $q = 1$ decays under the action of constant viscosity. In this case we have $b = 0$, so $y = \text{const}$. This means that the spectra collapse onto a single graph when $E(k, t, \nu)$ is divided by k^q ($= k$ in this case, because $q = 1$) and k is multiplied by t^a ($= t^{1/2}$ in this case). This is indeed the case, see the lower panel of Fig. 1.

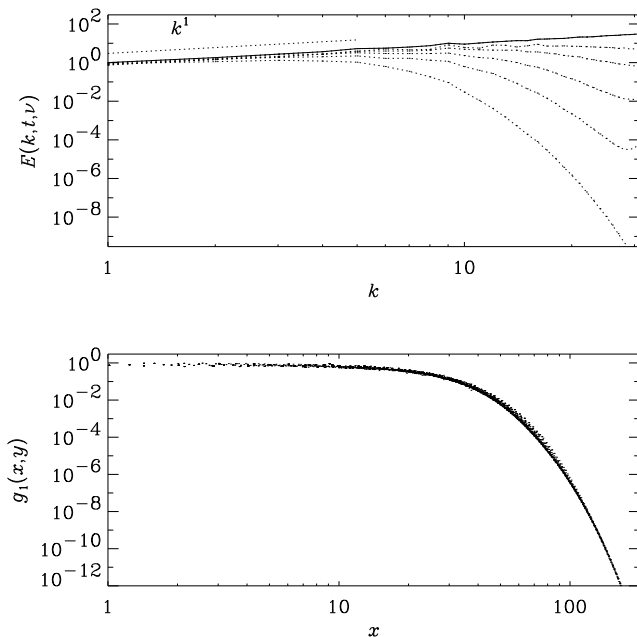


FIG. 1: Decay of the initial energy spectrum $E(k, 0, \nu) \sim k^q$ for $q = 1$ (upper panel) and the corresponding scaling function $g_q = E(k, t, \nu)/k^q$ versus $x = kt^a$ (lower panel). Note the collapse of the rescaled spectra for different times ($t = 0, 1, 2.5, 6, 12.5$, and 29). For $q = 1$ the parameter $a = 1/2$.

For all other values of q , the second argument, $y = \nu t^b$, will not be constant and must depend on t . We therefore expect that the spectrum will not collapse onto a single graph. This is shown in Fig. 2, where we show the spectra at different times (upper panel) and the attempt to collapse them onto a single graph (lower panel).

Collapse of the spectra obtained at different times is in general not possible unless one makes ν time-dependent in such a way as to keep $y = \nu(t)t^b$ constant in time. In the following simulations the viscosity is therefore given by

$$\nu(t) = \begin{cases} \nu_{\text{ref}} & \text{for } t \leq t_{\text{ref}}, \\ \nu_{\text{ref}} (t/t_{\text{ref}})^{-b} & \text{otherwise,} \end{cases} \quad (11)$$

where $\nu_{\text{ref}} = \nu(t_{\text{ref}})$ is a constant reference viscosity. At early times, $t < t_{\text{ref}}$, the initial fields were allowed to decay under the action of a constant viscosity, ν_{ref} , so

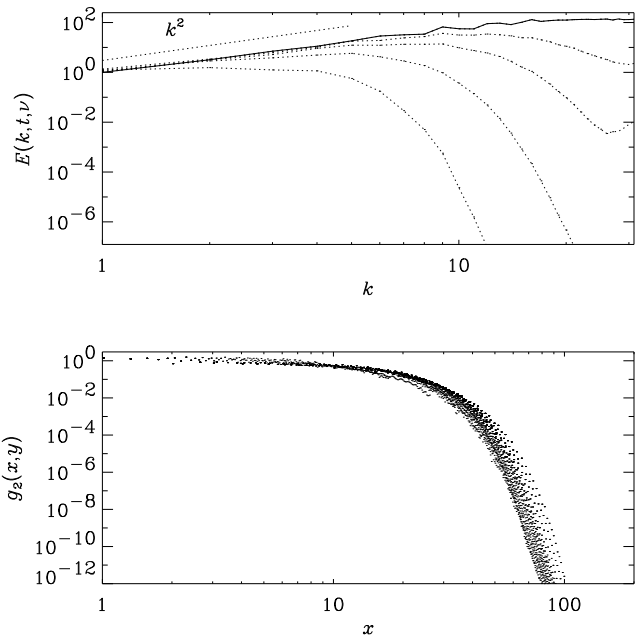


FIG. 2: Same as Fig. 1, but for $q = 2$ and constant viscosity, $\nu = 10^{-3}$. The times shown in the upper panel are $t = 0, 3, 9, 26$ and 77 . Note that the curves for different times do not collapse onto a single graph.

as to avoid having to use an excessively large (or even infinite) viscosity. The result is shown in Fig. 3 and the spectra for the different times collapse reasonably well onto a single graph.

B. Dependence of $g(x, y)$ on the first argument

It turns out that for a fixed value of y and different values of q the scaling function $g(x, y)$ does not quite collapse onto a single graph and that, therefore, the curves for different values of q are distinct. We indicate this by a subscript q and write $g_q(x, y)$. However, empirically it turned out that to a good approximation the q -dependence can be removed by rescaling x by a q -dependent factor, i.e.

$$x \rightarrow \tilde{x} = x(q+4)/5. \quad (12)$$

Note that for $q = 1$ we have $\tilde{x} = x$. In Fig. 4 we show $g_q(\tilde{x}, y)$ versus \tilde{x} for fixed value of y and three different values of q ($= 1, 2$, and 3). Note that the collapse of the three curves is reasonably good.

C. Modified time-dependence of viscosity

In order to verify the anticipated scaling behavior further, we determine effective values of q and check whether these values are consistent with each other. We begin by

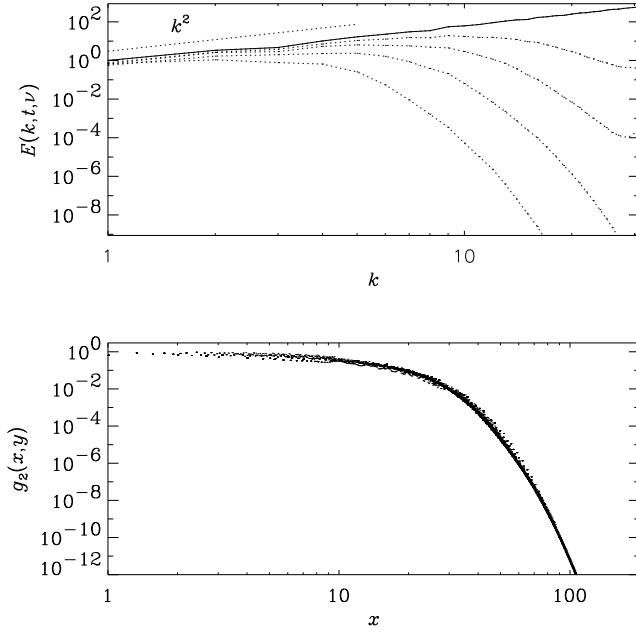


FIG. 3: Same as Fig. 2, but with $\nu = \nu(t)$ given by Eq. (11) with $\nu_{\text{ref}} = 3 \times 10^{-3}$ and $t_{\text{ref}} = 0.1$. Note that now the data points collapse reasonably well onto a single graph. In this figure the times are the same as in Fig. 2.

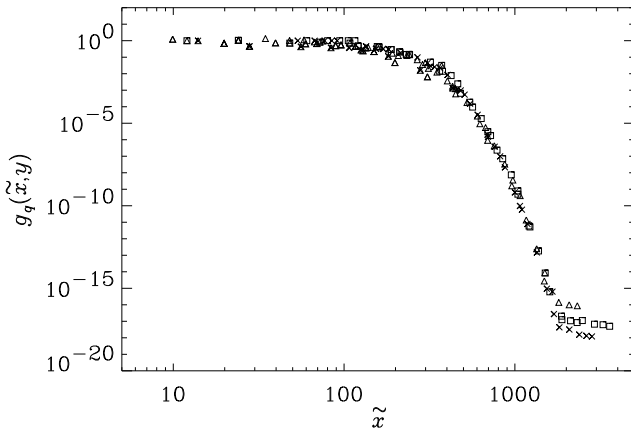


FIG. 4: Three sets of $g(\tilde{x}, y)$ curves from decay experiments with different values of q but the same value of $y = (2 \times 10^{-2})$. The abscissa has been rescaled according to Eq. (12) to make the curves for $q = 1$ (triangles), $q = 2$ (squares), and $q = 3$ (crosses) collapse onto a single graph.

defining an effective value q_ν that determines the time dependence of $\nu(t)$. Thus, $\nu(t)$ is proportional to t^{b_ν} where $b_\nu = -(1 - q_\nu)/(3 + q_\nu)$, which is analogous to Eq. (9). The result is shown in Fig. 5 and we see that the best collapse is indeed achieved when $q = q_\nu$. We have checked that this agreement holds also for different values of q .

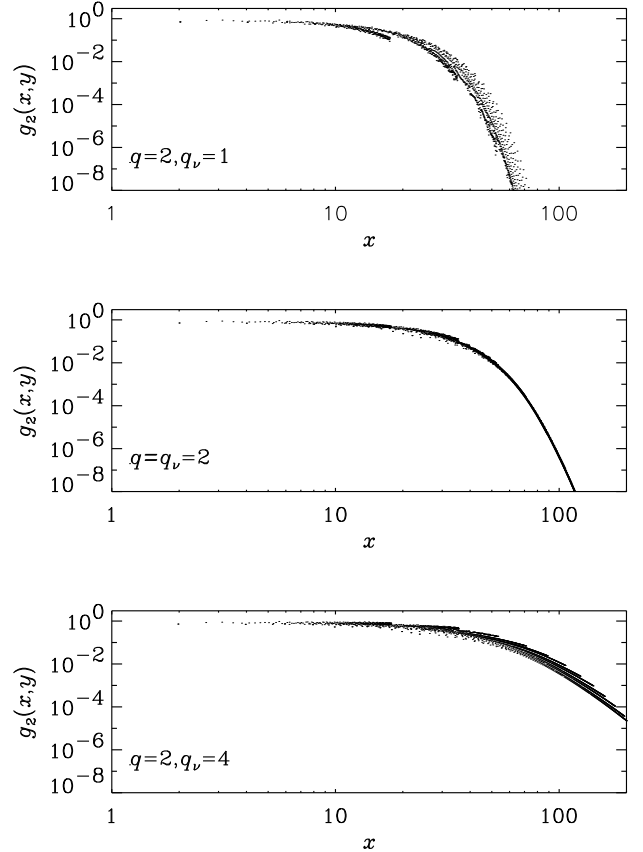


FIG. 5: Scatter plots for $q = 2$ and different values of q_ν . Note that the best collapse is achieved for $q_\nu = q$.

D. Dependence of $g_q(x, y)$ on the second argument

Next we consider the temporal decay law of the kinetic energy. This allows us to constrain the dependence of $g(x, y)$ on y . As usual, the kinetic energy (per unit mass and unit volume) can be found by integration,

$$E_{\text{kin}}(t, \nu) = \int_0^\infty E(k, t, \nu) dk \quad (t > 0). \quad (13)$$

For given value of y , where y may still be a function of t , Eq. (13) can be rewritten as an integral over the first argument of the scaling function, $x = kt^a$. This gives

$$E_{\text{kin}}(t, y) = t^{-a(1+q)} \int_0^\infty x^q g_q(x, y) dx, \quad (14)$$

where E_{kin} still depends on $y = y(t)$. Here we have ignored the fact that in order for $g_q(x, y)$ to be independent of q we should rescale the x coordinate by a factor $(q+4)/5$; see Eq. (12). However, this only corresponds to an overall rescaling of the kinetic energy by a factor $[(q+4)/5]^{-(q+1)}$ and is therefore unimportant.

It is convenient to isolate the main t -dependence,

$E_{\text{kin}} \sim t^{-2n}$, where $2n = a(1 + q)$, and

$$n = \frac{1 + q}{3 + q}. \quad (15)$$

We can therefore write

$$E_{\text{kin}}(t) \sim t^{-2n} \tilde{g}_q(\nu t^b), \quad (16)$$

where $\tilde{g} = \tilde{g}(y)$ is a function that only depends on one argument and is obtained by integrating out the x -dependence of $g(x, y)$, i.e.

$$\tilde{g}_q(y) = \int_0^\infty x^q g_q(x, y) dx. \quad (17)$$

The resulting values of $2n$ are given in Table I for different values of q . Note that the basic t^{-2n} decay law has also been obtained in Ref. [7], but there it was assumed that ν is negligibly small and that for large values of k one has a Kolmogorov spectrum. The basic relation between $2n$ and h or q can also be obtained by assuming that the rate of dissipation is proportional to v_l^3/ℓ , where ℓ is the integral scale [3].

In Fig. 6 we check that the basic decay law is indeed mostly governed by the value of q and not by the value of q_ν . For $q_\nu = q = 2$ the decay has the expected slope $2n = 1.2$ (middle panel). For $q_\nu = 1$, the viscosity is constant and the decay is accelerated, while for $q_\nu = 4$, the viscosity decreases faster than is necessary for keeping y constant and the decay of E_{kin} is now slower than what is expected based on the value of q . These results confirm that the best agreement is achieved for $q_\nu = q$. We have checked that the same is true for $q_\nu = q = 3$, for example.

We now turn to the y -dependence of $\tilde{g}_q(y)$, which can be determined by plotting $t^{2n} E_{\text{kin}}$ versus y ; see Fig. 7. Within plotting accuracy the results seem to be independent of the value of q . We can therefore drop in the following the subscript q on $\tilde{g}_q(y)$.

The results confirm that for small values of ν the time dependence of the decay law of kinetic energy is weaker: $\tilde{g} \sim y^{-0.85}$ for $y < 0.003$ compared to $\tilde{g} \sim y^{-1.8}$ for larger values of y . However, there is as yet no evidence that \tilde{g} becomes completely independent of y when $y \rightarrow 0$.

The above results imply that the energy decay law is attenuated by a small correction factor for $q \neq 1$. Consider, as an example, the case $q = 2$. The basic decay law is $E_{\text{kin}} \sim t^{-1.2}$, see Eq. (16). For $q = 2$ we have $b = 1/5$, so for small values of ν (assuming $y < 0.003$) the exponent has to be corrected by $-0.85/5 = -0.17$, so that the correct decay law is $E_{\text{kin}} \sim t^{-1.37}$. This is indeed confirmed by direct inspection of the data.

The fact that \tilde{g} does not seem to go to a finite value in the limit $y \rightarrow 0$ is surprising, because it implies that there is a viscosity correction to the basic t^{-2n} decay law even in the limit of vanishing viscosity. Although the data do not necessarily allow such an extrapolation, we are not aware of any evidence against a finite viscosity correction in the large Reynolds number limit.

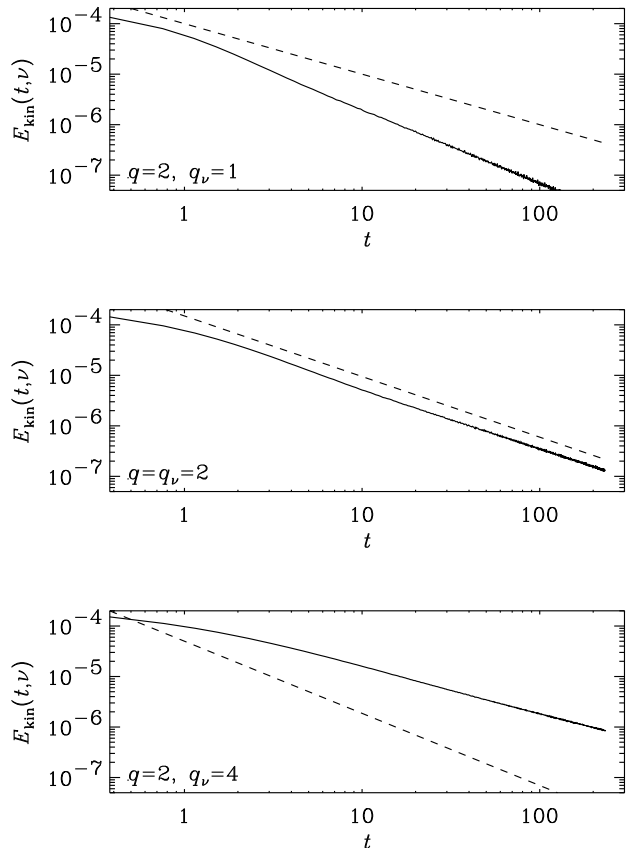


FIG. 6: Energy decay law for $q = 2$ and different values of q_ν (solid lines). The different slopes are $2n = 1.5, 1.2$, and 0.9 . The dashed lines indicate the slope expected if the decay law was governed by the value of q_ν (slopes 1, 1.2, and 1.43; see Table I). Again, the best collapse is achieved for $q_\nu = q$, corresponding to $2n = 1.2$.

E. Turbulent initial conditions

The results shown in the previous sections demonstrate that the scaling law (3) successfully describes the decay of kinetic energy in the special case of a flow field with an initial k^q spectrum. A more realistic initial condition is a turbulent velocity field which has an energy spectrum that is decreasing with increasing k . Nevertheless, there is always a subinertial range where values of q between 1 and 4 are not uncommon.

In the following we consider the decay of flow fields that are initially statistically stationary. These initial fields are produced by applying a random force within a band of wavenumbers around k_f until the work done by the forcing is balanced by dissipation. Relatively high resolution (256^3) and large values of k_f are needed in order to get a well-defined subinertial range.

As explained in §II, the scaling law Eq. (4) is a direct consequence of the scaling properties of the unforced Navier-Stokes equations, Eq. (5), and will not be valid for

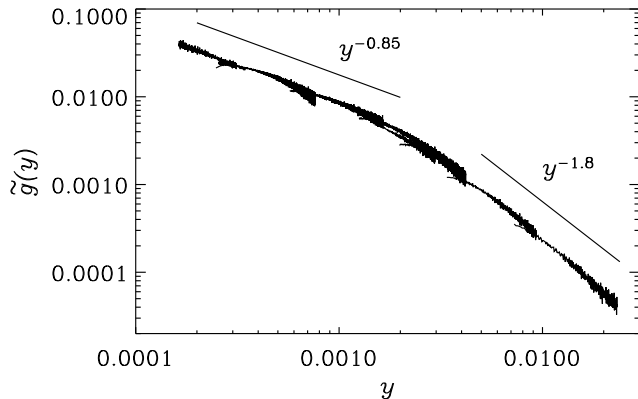


FIG. 7: Representation of $\tilde{g}_q(y)$ obtained by patching together the decay laws from different runs with different values of q . At early times the decay is not yet self similar, so the data for these times have been ignored in the plot (the remains of the initial transients can still be seen as little hooks in the beginning of each piece). Each piece of the decay curve has been shifted along the ordinate to connect the different pieces with each other. The normalization of \tilde{g} is therefore arbitrary.

a flow driven by a general forcing function. The statistically stationary state considered here will not necessarily be compatible with the Navier-Stokes equations. In the following we assume that $t = 0$ is the time when the forcing is stopped, but we must expect there to be some readjustment phase before self-similar scaling is possible.

When viscosity can be considered negligible or when it is made time-dependent according to Eq. (11), the parameter q can, in principle, be determined by two independent methods. It can be found by determining the spectral slope in the subinertial range or by fitting the energy decay to Eq. (16), as done in Ref. [7]. In addition, of course, q could be found completely empirically by trying different values until the collapse is best. Unfortunately the first approach is difficult since one has to have large scale separation between the size of the box and the integral (or forcing) scale in order to be able to resolve the infrared region. This requires very large resolution. In addition, the infrared limit obtained from simulations is not very accurate for small k , because only a few modes contribute to the shell-integrated spectrum.

In Fig. 8 we show the result for a turbulence simulation that was driven at $k_f = 10$ and the forcing was turned off at $t = 0$. Note that the collapse is relatively poor at early times. The collapse improves significantly when the turbulence is driven at $k_f = 30$; see Fig. 9.

The reason for the collapse being much better in the case of larger k_f is probably related to the facts that the local turnover time, $\tau_k \sim (u_{\text{rms}}\ell)^{-1}$, is shorter. Thus, self-similarity can probably commence much earlier.

Finally, we note that in our simulations the subinertial range slope is $q = 1.5$ both for large and small values

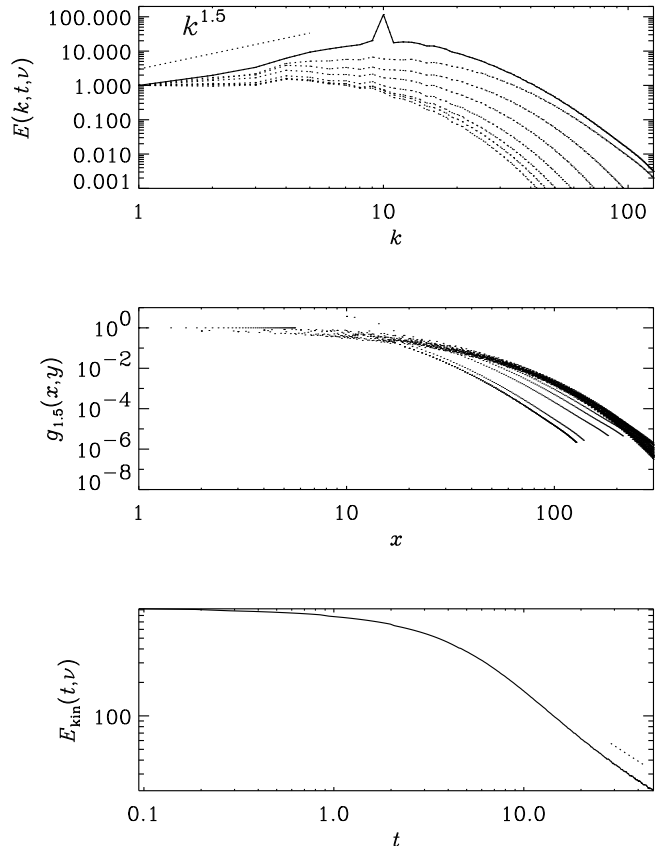


FIG. 8: Upper panel: initial energy spectrum (solid line) together with subsequent energy spectra (dotted lines) obtained from driven turbulence simulation forced at wavenumber $k_f = 10$. The spectral slope for small wavenumbers corresponds to $q = 1.5$. Middle panel: attempt to collapse the spectra on a single graph which fails at early times. Lower panel: decay of kinetic energy corresponding to a slope $2n = 10/9 \approx 1.11$, confirming the $q = 1.5$ scaling.

of k_f . We are not aware of a theoretical explanation for this slope, but it is probably related to finite size effects. By contrast, in an infinite domain the slope is expected to be $q = 4$ (or $= 2$), which could be motivated if the Loitsyansky (or Saffman) integral were independent of time. In that case one would have $2n = 10/7$ (or $2n = 6/5$).

F. Conclusion

The results presented above have shown that decaying hydrodynamic turbulence can be characterized by a two-parametric scaling function and that this function may well be universal and independent of the initial slope q of the spectrum in the infrared limit, i.e. in the subinertial range. Although the basic scaling behavior has already been confirmed earlier [7], using

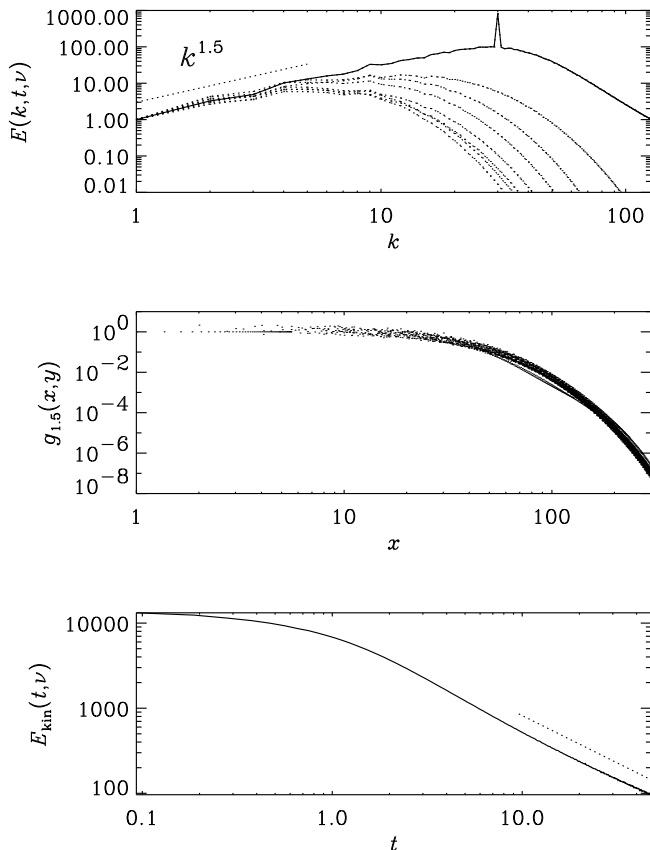


FIG. 9: Same as Fig. 8, but for $k_f = 30$. Note that the collapse is much better – even at earlier times – than for the case with $k_f = 10$ (middle panel).

data from wind tunnel turbulence [6], it was not possible to determine the infrared scaling properties of the energy spectrum. Indeed, for the smallest wavenumbers available from the wind tunnel data the spectrum was still a decreasing function of wavenumber k . This is because wind tunnel measurements only allow access to one-dimensional spectra which are always monotonically decaying. This property follows from the fact that for isotropic turbulence the three-dimensional spectrum $E(k)$ is related to the one-dimensional spectrum $E_{1D}(k)$ via $E(k) = -kdE_{1D}/dk$, and since $E(k) > 0$ it follows that the one-dimensional spectrum can never increase with k ; see Eq. (7) of Ref. [10]. This is also true

for the longitudinal and transversal power spectra separately; see, for example, Fig. 6.11 of Ref. [11]. Whether or not the proper subinertial range of the three-dimensional spectrum can be determined from wind tunnel experiments is unclear. It is therefore important that simulations can now demonstrate explicitly that the slope of the subinertial range spectrum is linked to the scaling law derived in Ref. [7].

There are obvious extensions of this work to the case of decaying magnetohydrodynamics turbulence. Similar scaling properties also apply to the magnetic case [12, 13], but the detailed functional dependence of the corresponding two-parametric scaling function has not yet been fully determined, although partial results do already exist. In particular, for the case of helical initial fields the combined dependence on wavenumber and time has been studied in Ref. [14], and resistive corrections to the decay law have been investigated in Ref. [15]. This work generalizes earlier findings that in the helical case the magnetic energy can decay as slowly as $\sim t^{-1/2}$ [16], while in the nonhelical case the decay is generally faster and similar to the hydrodynamic case [17].

A general difficulty with the self-similarity approach is the uncertainty regarding the zero point of t . There is apparently no unique way of determining this time a priori. An a priori choice of the zero point of t is however necessary if ν is allowed to be a function of time. Although the uncertainty regarding the zero point of t becomes less influential at later times, it is not normally possible to revise the zero point of t afterwards, unless one is prepared to run an entirely new simulation.

Once the initial startup phase is over and the decay has become self similar, one is however able to determine in full detail the exact form of the two-parametric scaling law. Our current work can only be preliminary, because it remains to be checked how general and perhaps even universal the $g(x, y)$ function really is. If its generality is established, it could become a powerful analysis tool for making predictions about the decay of kinetic energy. This applies in particular to the function $\tilde{g}(y)$, which plays the role of a viscosity dependent correction function for the decay law of the kinetic energy.

Acknowledgments

We acknowledge the use of the parallel computers in Trondheim, Odense, and Bergen.

-
- [1] B. B. Mandelbrot, *J. Fluid Mech.* **62**, 331 (1974).
 - [2] A. N. Kolmogorov, *C. R. Acad. Sci. URSS* **30**, 301 (1941)
 - [3] U. Frisch *Turbulence. The legacy of A. N. Kolmogorov.* Cambridge University Press (1995).
 - [4] J. O. Hinze *Turbulence.* McGraw-Hill: New York (1975).
 - [5] M. Lesieur *Turbulence in Fluids.* Martinus Nijhoff Publishers (1990).

- [6] G. Comte-Bellot and S. Corrsin, *Phys. Fluids* **48**, 273 (1971).
- [7] P. D. Ditlevsen, M. H. Jensen, and P. Olesen, arxiv.org/abs/nlin.CD/0205055 (2002).
- [8] www.nordita.dk/data/brandenb/pencil-code
- [9] Williamson, J. H. , *J. Comp. Phys.* **35**, 48 (1980).
- [10] W. Dobler, N. E. L. Haugen, T. A. Yousef, and A. Bran-

- denburg, Phys. Rev. **E 68**, 026304 (2003).
- [11] S. B. Pope *Turbulent flows*. Cambridge: Cambridge University Press (2000).
- [12] P. Olesen, Phys. Lett. **B 398**, 321 (1997).
- [13] C. Kalelkar and R. Pandit, arxiv.org/cond-mat/0307243 (2003).
- [14] M. Christensson, M. Hindmarsh, and A. Brandenburg, Phys. Rev. **E 64**, 056405 (2001).
- [15] M. Christensson, M. Hindmarsh, and A. Brandenburg, arxiv.org/astro-ph/0209119 (2002).
- [16] D. Biskamp and W.-C. Müller, Phys. Rev. Lett. **83**, 2195 (1999).
- [17] M.-M. Mac Low, R. S. Klessen, and A. Burkert, Phys. Rev. Lett. **80**, 2754 (1998).